Proceedings of the 2009 American Control Conference, St. Louis, MO, June 2009

On the Trajectories and Coordination of Steered Particles with Time-Periodic Speed Profiles

Daniel T. Swain, Naomi Ehrich Leonard

***Abstract*— Motivated by observations of fish and possibilities for mobile robotics, we study collective motion of networks of agents that move with periodically time-varying speed. Each agent is modeled as a particle with constant turning rate and time-periodic speed profile at steady state. Expressions are derived for the trajectories of such particles, emphasizing the variation from the constant-speed circular orbit. We show that trajectories remain bounded if the speed profile contains no frequency content at the turning rate. Steering and speed control laws are derived that stabilize a rich family of collective motion patterns of a many-particle system about a common center point, where headings and speed phases are coordinated.**

I. INTRODUCTION

It has proved useful in the study of collective motion and coordinated control to model individual agents as steered particles in the plane with constant speed or velocity constraints. Such a model yields a relatively simple framework for design and analysis of coordinating control laws. This model has been readily adopted in practice because it can be used to capture the group-level interconnection and motion coordination dynamics central to organizing a variety of mobile robotic networks, including autonomous underwater vehicles [1] and aerial vehicles [2]. Work by Vicsek [3] may be seen as a historical precedent with an array of analytic work that followed, including [4], [5]. The steered particle model has also been utilized in the study of biological collective motion, for example in the schooling of fish [6].

In this paper we consider a steered particle model that is augmented with a periodically time-varying speed. We extend and make more precise results presented in [7]; there we considered trajectories and coordination of agents with purely sinusoidal time-varying speed motivated by observations of fish that exhibit coordinated behavior involving speed modulation. Our continued investigation is motivated both by further inquiry of the observed fish behavior and by the promising possibilities for application of modulation in the particle model to mobile robotic networks. In [8] benefits of speed modulation to connectivity and consensus dynamics are discussed. In [9], [10] heading is modulated to obtain a degree of small-time local controllability.

In the patterns stabilized in this paper, particles regularly vary their position within the group while maintaining an overall formation shape. This enables a network of mobile sensors to obtain spatially-separated samples consistently over time. In particular, every agent repeatedly rotates its position within the group so that it is on the "inside", "outside", "front", and "back" of the formation, thereby providing a level of redundancy to the sampling process and possibly benefiting estimation applications [1]. Likewise, it may be advantageous in the context of fish schools for individual fish to regularly exchange roles or vary position within the school's spatial domain. We note also that collisions are avoided in the steady-state patterns for agents that are small in size relative to the scale of the formation.

In this paper we describe the steady-state trajectories of steered particles with time-periodic speed profiles and systematically derive control laws to stabilize formations of N identical agents. We generalize to allow some heterogeneity among agents. Our control laws stabilize the motion of the particles about a common "center" (a notion we make precise) with coordinated headings and speeds. The steady-state headings and speeds correspond to critical points of potential functions defined over the torus T^N. The approach follows that of [11] applied to an augmented model that allows for periodic speed variation.

In Section II we describe the model and notation. We describe the resulting open-loop trajectories in Section III. In Section IV we derive steering and speed feedback control laws to stabilize a large class of motion patterns.

II. STEERED PARTICLE MODEL WITH PERIODIC SPEED

We consider N unit-mass particles moving in the plane, which we identify with the complex plane; that is, $\mathbb{C} \sim \mathbb{R}^2$. The position of particle k is $r_k \in \mathbb{C}$, its heading with respect to the real axis is $\theta_k \in S^1$. Particle k is assumed to have speed $\alpha_k(t) = 1 + v_k(t)$ where $v_k : \mathbb{R} \to (-1, 1)$. The dynamics are given by

$$\dot{r}_k = (1 + v_k(t))\, e^{i\theta_k} \tag{1}$$

$$\dot{\theta}_k = \omega + u_k, \tag{2}$$

where ω is a constant turning rate and u_k is a steering control that is zero at steady state.

Although it is not strictly required for several of the results in this paper, we will generally consider v_k to be a 2π-periodic and zero-mean function of a time-varying *speed phase* $\phi_k \in S^1$. When this is the case, we may write $v_k(\phi_k)$, such that $v_k(\phi_k) = v_k(\phi_k + 2\pi)$. The speed phase dynamics are given by

$$\dot{\phi}_k = \Omega + g_k, \tag{3}$$

where Ω is a constant describing the intrinsic rate of change of the speed phase and g_k is a speed phase control that is

D.T. Swain and N.E. Leonard are with the Mechanical and Aerospace Engineering Department, Princeton University, Princeton, NJ 08544 USA, {dswain}{naomi}@princeton.edu

zero at steady state. We refer to ω and Ω as the *natural frequencies* of heading and speed phase, respectively.

We use a boldface notation to represent the ordered vector of the corresponding subscripted quantity, for example,

$$\mathbf{r} = \begin{bmatrix} r_1 & \cdots & r_N \end{bmatrix}^T \in \mathbb{C}^N$$

and

$$\boldsymbol{\theta} = \begin{bmatrix} \theta_1 & \cdots & \theta_N \end{bmatrix}^T \in T^N.$$

For complex vectors $\mathbf{z}_1, \mathbf{z}_2 \in \mathbb{C}^M$, $M \in \mathbb{Z}^+$, we denote $\bar{\mathbf{z}}_1$ to be the complex conjugate of $\mathbf{z}_1$ and use the inner product $\langle \mathbf{z}_1, \mathbf{z}_2 \rangle = \mathrm{Re}\left\{\mathbf{z}_1^T \bar{\mathbf{z}}_2\right\}$.

The headings and speed phases of the group both evolve on T^N, hence it is convenient to use concepts from the coupled oscillator literature (e.g. [12], [13]). We briefly review the key concepts and notation here; for a more complete review see [14]. Consider a general set of phases $\boldsymbol{\psi} \in T^N$. The complex order parameter p_ψ is defined by

$$p_\psi = \frac{1}{N} \sum_{k=1}^{N} e^{i\psi_k}, \tag{4}$$

with the property that $|p_\psi|^2 = 1$ when the phases are *synchronized* ($\psi_1 = \psi_2 = \ldots = \psi_N$ modulo 2π). When $|p_\psi|^2 = 0$, we say that the phases are *balanced*. The *splay state* (evenly spaced phases) is a special case of a balanced arrangement.

The following class of potential functions is useful in the present context.

Definition 1: (*Phase Potentials*) Consider the class $\mathcal{P}$ of C^2 functions on T^N defined such that, for any $U \in \mathcal{P}$, 1) $U : T^N \to [0, U_{max}]$ for some scalar $U_{max} > 0$, and 2) $\langle \mathrm{grad}\ U, \mathbf{1}_N \rangle = 0$ where $\mathbf{1}_N \in \mathbb{R}^N$ is the vector of all ones. We call an element of $\mathcal{P}$ a *phase potential*.

For any $U(\boldsymbol{\psi}) \in \mathcal{P}$, when $\dot{\psi}_k = \dot{\psi}$ for each $k = 1, \ldots, N$ and $\dot{\psi}$ is constant, we have (because $\langle \mathrm{grad}\ U, \mathbf{1}_N \rangle = 0$)

$$\frac{d}{dt} U(\psi) = \frac{d}{dt} \frac{\partial U}{\partial \psi_k} = 0. \tag{5}$$

III. ANALYSIS OF OPEN-LOOP TRAJECTORIES

Here we derive the trajectories traced out by particles evolving in the open-loop case with the dynamics (1)-(3), that is, when $u_k = g_k = 0$. The case of $\omega = 0$ results in straight-line motion, important for translational motion of the group [14], [8]. In the following we assume that $\omega \neq 0$.

First, we study boundedness of the trajectories and derive an important condition for the admissible frequency content of the particle speed profile.

Theorem 1: (*Boundedness of Trajectories*) The trajectory of a particle with dynamics described by (1)-(3) with $\omega \neq 0$ and $u_k = g_k = 0$ is bounded if v_k is a bounded function of time and

$$\left| \int_0^\infty v_k(\tau) e^{i\omega\tau} d\tau \right| = |V_k(s)|_{s=i\omega} \tag{6}$$

is bounded, where $V_k(s)$ is the Laplace transform of $v_k(t)$. That is, the trajectory is bounded as long as v_k has no $2\pi/\omega$-periodic components.

Proof: Note first that when $\omega = 0$ the result is unbounded straight-line motion. When $\omega \neq 0$, the trajectory may be found by simply integrating (1), giving

$$r_k = C_k - i\omega^{-1} e^{i\theta_k(t)} + \int_0^t v_k(\tau) e^{i\theta_k(\tau)} d\tau \tag{7}$$

for some constant $C_k \in \mathbb{C}$. The magnitude of r_k remains bounded as long as the integral term remains bounded in magnitude. Because v_k is bounded, the integral may only grow unbounded in the limit $t \to \infty$. Substitute the heading, given by $\theta_k(t) = \omega t + \theta_k(0)$, into (7). The magnitude of the resulting integral is bounded for $t \to \infty$ when (6) is bounded. ■

In the case that v_k is a periodic function of ϕ_k and hence $2\pi/\Omega$-periodic in time, we have the following.

Corollary 1: (*Boundedness of Trajectories - Periodic Speed Profile*) For the setup of Theorem 1 with v_k a 2π-periodic function of the speed phase ϕ_k, the trajectory r_k is bounded if there is no integer ℓ such that both $\ell\Omega = \omega$ and $V_k(\ell\Omega) \neq 0$. That is, v_k may not contain any harmonics at the frequency ω.

Proof: This follows immediately from Theorem 1. ■

It is straightforward to see that constant speed, i.e., $v_k = 0$, results in a circular trajectory. We describe such a trajectory by writing

$$r_k = c_k + R(\theta_k) \tag{8}$$

where $c_k \in \mathbb{C}$ is a constant center of the orbit and

$$R(\theta_k) = -i\omega^{-1} e^{i\theta_k} \tag{9}$$

describes a circle of radius ω^{-1}. We extend this decomposition to account for variations in speed.

Definition 2: (*Nonconstant Speed Trajectory Decomposition*) The trajectory traced out by a particle under dynamics (1)-(3) with $u_k = g_k = 0$ is described by the decomposition

$$r_k = c_k + R(\theta_k) + q_k(\phi_k) e^{i\theta_k}, \tag{10}$$

where $R(\theta_k)$ is defined by (9) and q_k is defined so that c_k is a constant of the motion. This requires q_k to satisfy the differential relationship

$$\frac{d}{dt} q_k + i\omega q_k = v_k. \tag{11}$$

Furthermore, $q_{k0} := q_k(\phi_k(0))$ is chosen so that

$$\int_0^\infty q_k(t) \bar{z}(t) dt = 0, \ \forall z(t) \in \mathcal{N}(L), \tag{12}$$

where $\mathcal{N}(L)$ is the null space of the operator

$$L : q \mapsto \dot{q} + i\omega q. \tag{13}$$

This ensures that q_k contains only the particular solution to (11) and hence $R(\theta_k)$ accounts for the entirety of the motion resulting from the constant turning rate ω. Within this setting, we say that c_k is the *center of the trajectory*.

The following allows us to find the value of q_{k0} that satisfies Definition 2.

Lemma 1: The initial condition

$$q_{k0} = -\left. V_k(s)\right|_{s=-i\omega}, \tag{14}$$

where $V_k(s)$ is the Laplace transform of $v_k(t)$, satisfies Definition 2.

Proof: We have $\mathcal{N}(L) = \text{span}\left\{e^{-i\omega t}\right\}$ and therefore (12) is satisfied if

$$\int_0^\infty q_k(t)e^{i\omega t}dt = \left. Q_k(s)\right|_{s=-i\omega} = 0,$$

where $Q_k(s)$ is the Laplace transform of $q_k(t)$. From (11) we have

$$sQ_k(s) - q_{k0} + i\omega Q_k(s) = V_k(s)$$

and by evaluating at $s = -i\omega$ we obtain (14). ∎

Note that (11) may be rewritten in steady state as

$$\Omega q_k' + i\omega q_k = v_k \tag{15}$$

where $q_k' = \frac{\partial q_k}{\partial \phi_k}$.

Consider a complex coordinate frame with origin at $c_k + R(\theta_k)$ and oriented with θ_k along its positive real axis. This rotating frame is equivalent to the body-fixed, velocity-oriented, frame of a particle sharing the same c_k and θ_k as particle k, but with constant unit speed. The locus of all points $q_k(\phi)$ for $\phi \in S^1$ describes a smooth curve that is invariant in the rotating constant-speed frame, with the point $q_k(\phi_k)$ being the location of particle k in this frame. One may view q_k as describing a curve in this frame and ϕ_k as parameterizing the location of particle k along this curve. Fig. 1 illustrates this concept and shows the ellipsoidal locus of q_k for purely sinusoidal speed, which we now derive.

Lemma 2: (*Trajectory Resulting from Sinusoidal Speed Profile*) Under the dynamics (1)-(3) with $u_k = g_k = 0$, $\omega \neq 0$, $\Omega \neq 0$, $\Omega \neq \omega$, and speed profile described by

$$v_k = \mu_k \cos\left(\phi_k - \varphi_k\right) \tag{16}$$

for constants $\mu_k \in (0, 1)$ and $\varphi_k \in S^1$, the trajectory decomposition described by (10) can be written with either of the following equivalent forms for q_k:

$$q_k = \frac{-\Omega v_k' + i\omega v_k}{\Omega^2 - \omega^2} \tag{17}$$

$$= \mu_k \frac{\Omega \sin\left(\phi_k - \varphi_k\right) + i\omega \cos\left(\phi_k - \varphi_k\right)}{\Omega^2 - \omega^2} \tag{18}$$

where $v_k' = \frac{\partial v_k}{\partial \phi_k}$.

Proof: To satisfy (11) and (12), we write q_k in the general form of the particular solution as

$$q_k = A_k \cos\phi_k + B_k \sin\phi_k$$

for complex constants A_k and B_k. By writing (16) as

$$v_k = \mu_k \cos\varphi_k \cos\phi_k + \mu_k \sin\varphi_k \sin\phi_k$$

it is straightforward to plug into (15), solve for A_k and B_k, and rewrite in either of the forms above. ∎

We note that (17) matches the result given in [7], in the case $v_k = \mu \cos\phi_k$ (i.e. $\varphi_k = 0$). Also note that $q_k(0)$ given by (17) is equivalent to (14).

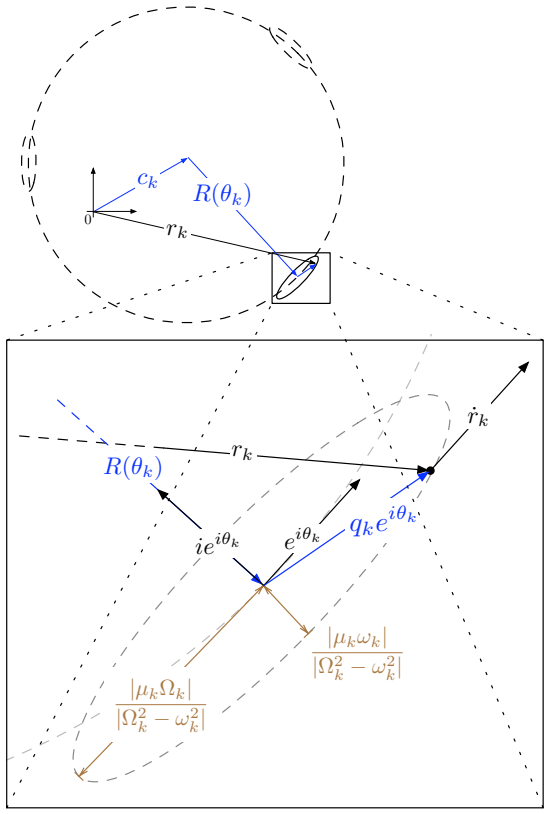

Fig. 1. Illustration of the decomposition (10) with sinusoidal speed profile yielding the solution (17). For this and more general speed profiles it is useful to consider the coordinate frame located at $c_k + R(\theta_k)$ with real axis in the direction $e^{i\theta_k}$. In the purely sinusoidal speed case, q_k traces out an ellipse in this frame (as shown).

The solution (17) traces out an ellipse with eccentricity $\frac{\omega}{\Omega}$ as ϕ_k cycles from 0 to 2π. The ellipse is bounded by the box defined by

$$\left|\text{Re}\left\{q_k\right\}\right| \leq \left|\frac{\mu_k\Omega}{\Omega^2 - \omega^2}\right|, \quad \left|\text{Im}\left\{q_k\right\}\right| \leq \left|\frac{\mu_k\omega}{\Omega^2 - \omega^2}\right|.$$

The ratio ω/Ω is of great importance to the shape of the resulting trajectory. A more extensive analysis is given in [7].

Lemma 2 leads to a straightforward extension allowing us to describe the steady-state trajectories for almost arbitrary periodic speed profiles with period $2\pi/\Omega$.

Theorem 2: (*Trajectory Resulting From General Periodic Speed Profile*) Consider a $2\pi/\Omega-$periodic speed profile which can be represented by the Fourier series

$$v_k = \sum_{\ell=1}^{\infty} \mu_{k,\ell} \cos\left(\ell\phi_k - \varphi_{k,\ell}\right) \tag{19}$$

for which there is no ℓ such that both $\ell\Omega = \omega$ and $\mu_{k,\ell} \neq 0$. The trajectory decomposition defined by Definition 2 is given by (10) with

$$q_k = \sum_{\ell=1}^{\infty} \mu_{k,\ell} \frac{\ell\Omega \sin\left(\ell\phi_k - \varphi_{k,\ell}\right) + i\omega \cos\left(\ell\phi_k - \varphi_{k,\ell}\right)}{\left(\ell\Omega\right)^2 - \omega^2}. \tag{20}$$

Proof: The form of the solution follows as an extension of Lemma 2 and the linearity of the operator L (13). The condition on harmonics is required to satisfy Corollary 1. ■

We may also extend the bounds on q_k to the general periodic case.

Corollary 2: If the periodic speed profile is of bounded root-mean-square (RMS) value, then the solution (20) is bounded as follows:

$$|\mathrm{Re}\{q_k\}| \leq v_k^{rms} \left(\sum_{\substack{\ell=1 \\ \mu_{k,\ell}\neq 0}}^{\infty} \left(\frac{\ell\Omega}{(\ell\Omega)^2 - \omega^2} \right)^2 \right)^{\frac{1}{2}} \quad (21)$$

$$|\mathrm{Im}\{q_k\}| \leq v_k^{rms} \left(\sum_{\substack{\ell=1 \\ \mu_{k,\ell}\neq 0}}^{\infty} \left(\frac{\omega}{(\ell\Omega)^2 - \omega^2} \right)^2 \right)^{\frac{1}{2}} \quad (22)$$

where

$$v_k^{rms} = \left(\frac{1}{2\pi} \int_{-\pi}^{\pi} v_k(\phi) d\phi \right)^{\frac{1}{2}} = \sum_{\ell=1}^{\infty} \mu_{k,\ell}^2$$

is the RMS value of v_k and the second equality is due to Parseval's theorem.

Proof: By assumption, v_k^{rms} is bounded. By the conditions for boundedness of the solution, there is no ℓ such that both $\ell\Omega = \omega$ and $\mu_{k,\ell} \neq 0$ and therefore the terms of the infinite sum in (21) are bounded and asymptotically approach $(\ell\Omega)^{-2}$. Likewise, the terms in (22) are bounded and asymptotically approach $\omega^2(\ell\Omega)^{-4}$. Hence both sums converge. The inequalities then follow from the Schwarz inequality. ■

Fig. 2 shows a sample speed profile with three randomly chosen harmonic modes. The shape of q_k is described by superposing a series of ellipses, one corresponding to each harmonic. The $\ell = 1$ ellipse is centered at the origin, the $\ell = 2$ ellipse is centered about a point on the $\ell = 1$ ellipse that cycles with frequency Ω, the $\ell = 3$ ellipse is centered about a point on the $\ell = 2$ ellipse that cycles with frequency 2Ω. In the figure there are only three modes, but in general this sequence would continue for each ℓ.

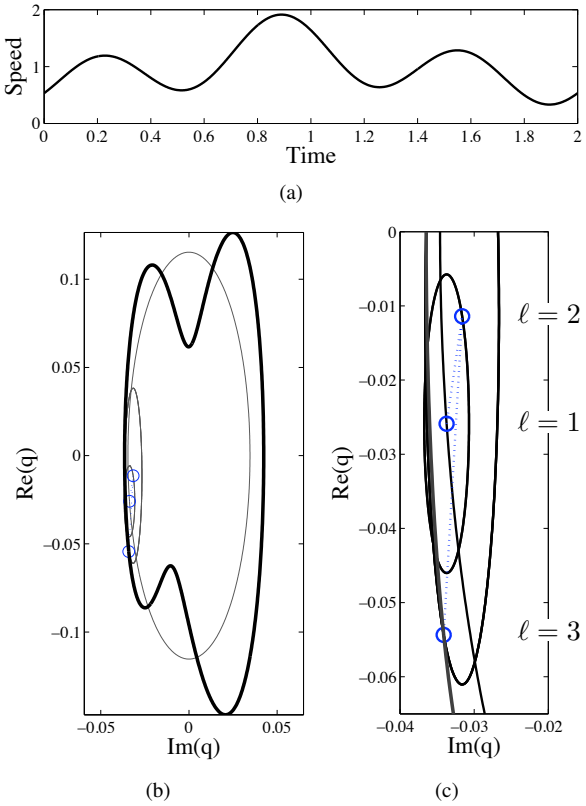

Fig. 2. (a) Periodic speed profile with $\Omega = \pi$ and three randomly generated harmonic components. (b) The corresponding q_k (black curve) as described by (20), with $\omega = 0.3\pi$. The gray curves are the individual ellipses corresponding to the terms in the sum - each superimposed on the previous - with a blue circle on each indicating the point corresponding to $t = 0$. That is, the $\ell = 1$ ellipse is centered at the origin with its $t = 0$ point marked with a blue circle, the $\ell = 2$ ellipse is centered about that point an so on. (c) is a zoomed version of (b). The middle blue circle corresponds to the point on the $\ell = 1$ ellipse at $t = 0$, the upper and lower blue circles similarly corresponding to $\ell = 2$ and $\ell = 3$ respectively.

IV. COORDINATION OF PARTICLES WITH PERIODIC SPEED PROFILES

In [14] and [7] the design approach parametrizes the desired steady-state trajectories of a set of particles and systematically derives stabilizing control laws to coordinate these trajectories. In [14], a methodology is developed to systematically stabilize spacing and phase coordination, where phase refers to the direction of motion of a particle θ_k. Phase coordination is achieved with a control term that corresponds to the gradient of a phase potential with critical points at the desired relative phase arrangement. Similarly the spacing control law minimizes a spacing potential; in the case of circular motion the particles provably converge to trajectories that share a common circular motion center. In [7] we proposed, without proof of stability, analogous control laws to stabilize motion patterns with coordination of spacing, heading (direction of motion) as well as phase of speed oscillations in the case of sinusoidal speed profiles. Here we derive and prove such stabilizing control laws for coordination of particles with general time-periodic speed profiles; the results specialize to the sinusoidal case studied in [7].

We extend the notion of the trajectory center c_k in (10) and define

$$c_k(t) := r_k(t) - R(\theta_k(t)) - q_k(\phi_k(t))e^{i\theta_k(t)} \quad (23)$$

as the *instantaneous center of the trajectory*, where q_k is taken to be the solution to (15). We have

$$\dot{c}_k = -u_k \left(\omega^{-1} + iq_k\right) e^{i\theta_k} + g_k\Omega^{-1} \left(v_k + i\omega q_k\right) e^{i\theta_k},$$

and hence $c_k(t)$ is constant when $u_k = g_k = 0$.

Consider the candidate Lyapunov function

$$S(\mathbf{r}, \boldsymbol{\theta}, \boldsymbol{\phi}) = \kappa_c \frac{1}{2} \|P\mathbf{c}\|^2 + \kappa_\theta U(\boldsymbol{\theta}) + \kappa_\phi V(\boldsymbol{\phi}) + S_0 \geq 0 \quad (24)$$

where $P = I_{N\times N} - \frac{1}{N}\mathbf{1}_N^T\mathbf{1}_N$, $\mathbf{1}_N$ is the N-vector of ones, $\kappa_c > 0$, κ_θ, and κ_ϕ are all real constants, U and V are

members of class $\mathcal{P}$, $S_0 = \min_{\boldsymbol{\theta},\boldsymbol{\phi}} \{\kappa_\theta U(\boldsymbol{\theta}) + \kappa_\phi V(\boldsymbol{\phi})\}$ is a constant that enforces $S \geq 0$, and we use the norm induced by the inner product on $\mathbb{C}^N$ as defined above. $P = P^T = P^2$ is a projector with kernel $\mathbf{1}_N$ and it is useful to note that $P_k\mathbf{x} = x_k - \frac{1}{N}\sum_{j=1}^N x_j$ where P_k is the k^{th} row of P and $\mathbf{x} \in \mathbb{C}^N$. Thus, $P\mathbf{c} = \mathbf{0}$ is equivalent to $c_k = c_0$ for some $c_0 \in \mathbb{C}$ and for all $k = 1, \ldots, N$. Note that S is bounded from below, with the actual bound depending on the signs of κ_θ and κ_ϕ and possibly the maximum potential values U_{max} and V_{max}.

The time derivative of S along trajectories of the dynamics (1)-(3) is given by

$$\dot{S} = \sum_{k=1}^{N} \left(\kappa_c \langle P_k\mathbf{c}, \dot{c}_k \rangle + \kappa_\theta \frac{\partial U}{\partial \theta_k} u_k + \kappa_\phi \frac{\partial V}{\partial \phi_k} g_k \right)$$

where we have used the property $\langle \text{grad } U, \mathbf{1}_N \rangle = \langle \text{grad } V, \mathbf{1}_N \rangle = 0$. Hence, choosing

$$u_k = \left(\kappa_c \omega^{-1} \left\langle P_k\mathbf{c}, (1 + i\omega q_k)\, e^{i\theta_k} \right\rangle - \kappa_\theta \frac{\partial U}{\partial \theta_k} \right) \quad (25)$$

and

$$g_k = -\left(\kappa_c \Omega^{-1} \left\langle P_k\mathbf{c}, (v_k + i\omega q_k)\, e^{i\theta_k} \right\rangle + \kappa_\phi \frac{\partial V}{\partial \phi_k} \right) \quad (26)$$

gives us

$$\dot{S} = -\sum_{k=1}^{N} \left(u_k^2 + g_k^2 \right) \leq 0. \quad (27)$$

We require the following to prove stability.

Lemma 3: (*Positively Invariant Sets*) For any $p > 0$ and S defined by (24), the set

$$W_p = \big\{ P\mathbf{x} \in \mathbb{C}^N, \boldsymbol{\theta} \in T^N, \boldsymbol{\phi} \in T^N : \mathbf{x} \in \mathbb{C}^N, S(\mathbf{x}, \boldsymbol{\theta}, \boldsymbol{\phi}) \leq p \big\}$$

is positively invariant under the dynamics (1)-(3) with controls (25) and (26). Furthermore, W_p is a compact subset of $D = \big\{ \text{Image } P \times T^N \times T^N \big\}$.

Proof: On W_p we have $\frac{\kappa_c}{2} \|P\mathbf{x}\|^2 \leq S(\mathbf{x}, \boldsymbol{\theta}, \boldsymbol{\phi}) \leq p$, hence W_p is a closed subset of $\big\{ A \times T^N \times T^N \big\} \subset D$ where $A = \left\{ z \in \text{Image } P : \|z\|^2 \leq \frac{2p}{\kappa_c} \right\}$ is a compact subset of Image P. Therefore $W_p \subset D$ is compact. (27) gives us positive invariance. ∎

Lemma 4: (*Invariant Sets on $\dot{S} = 0$*) Consider the set

$$\Lambda = \left\{ (\mathbf{r}, \boldsymbol{\theta}, \boldsymbol{\phi}) \in (C^N \times T^N \times T^N) : \dot{S}(\mathbf{r}, \boldsymbol{\theta}, \boldsymbol{\phi}) \equiv 0 \right\}.$$

Invariant sets on Λ are subsets of

$$M = \left\{ (\mathbf{r}, \boldsymbol{\theta}, \boldsymbol{\phi}) \in \Lambda : P\mathbf{c} = 0 \text{ and } \frac{\partial U}{\partial \theta_k} = \frac{\partial V}{\partial \phi_k} = 0,\ \forall k \right\}. \quad (28)$$

On M, $\dot{\theta}_k = \omega$ and $\dot{\phi}_k = \Omega$ for all k.

Proof: By (27), $\dot{S} \equiv 0$ implies $u_k \equiv g_k \equiv 0$ and hence $\dot{\theta}_k = \omega$, $\dot{\phi}_k = \Omega$. Therefore c_k is a constant for each k and so is $P_k\mathbf{c}$. $\dot{S} \equiv 0$ also implies $\frac{d}{dt} u_k \equiv 0$. Because $\dot{\theta}_k$ and $\dot{\phi}_k$ are constant, (5) holds and (25) with $u_k \equiv 0$ implies

$$\frac{d}{dt} \left\langle P_k\mathbf{c}, (1 + i\omega q_k)\, e^{i\theta_k} \right\rangle \equiv 0 \quad (29)$$

for each k. We have

$$\frac{d}{dt} \left\langle P_k\mathbf{c}, (1 + i\omega q_k)\, e^{i\theta_k} \right\rangle = \langle P_k\mathbf{c}, i\omega \dot{r}_k \rangle .$$

Since the velocity $\dot{r}_k$ is never zero, for (29) to hold for all t, we must have $P_k\mathbf{c} \equiv 0$. By (25) and (26) we must therefore also have

$$\frac{\partial U}{\partial \theta_k} = \frac{\partial V}{\partial \phi_k} = 0.$$

This describes the set M. ∎

We may now state the following.

Theorem 3: (*Main Stability Theorem*) For any initial condition, the dynamics (1)-(3) with controls (25) and (26) asymptotically converge to the invariant set M of Lemma 4. Thus, convergence is to trajectories as described by (10) with a common constant center $c_k = c_0$ for some $c_0 \in \mathbb{C}$, $\dot{\theta}_k = \omega$, and $\dot{\phi}_k = \Omega$ for all $k = 1, \ldots, N$. Phase arrangements of the θ_k correspond to critical points of U and phase arrangements of the ϕ_k correspond to critical points of V. Furthermore, maxima of U (V) are stable if $\kappa_\theta > 0$ ($\kappa_\phi > 0$) and minima of U (V) are stable if $\kappa_\theta < 0$ ($\kappa_\phi < 0$).

Proof: By (27) the value of S as defined by (24) is nonincreasing along solutions of the described dynamics. By Lemma 3 we can find a p so that the initial condition lives in a positively invariant compact subset W_p of $\big\{ \text{Image} P \times T^N \times T^N \big\}$. By the LaSalle Invariance Principle all solutions approach the largest invariant set on which $\dot{S} = 0$. By Lemma 4 this is the set M. The stability of maxima and minima of U (V) follows from the sign of the gradient terms in the control laws. ∎

The above result holds for any phase potentials U and V in $\mathcal{P}$. One choice of interest is the heading potential

$$U(\boldsymbol{\theta}) = \frac{1}{2} |p_\theta|^2 \quad (30)$$

where p_θ is defined by (4) and speed phase potential

$$V(\boldsymbol{\phi}) = \sum_{m=1}^{\lfloor \frac{N}{2} \rfloor} K_m \left| \frac{1}{mN} \sum_{k=1}^{N} e^{im\theta_k} \right|^2 . \quad (31)$$

In [14] it was shown that (30) has local minima only for synchronized headings, i.e., $\theta_k = \theta_0$ for all $k = 1, \ldots, N$ and some $\theta_0 \in S^1$. Also, when $K_m > 0$ for $m = 1, \ldots, \lfloor \frac{N}{2} \rfloor - 1$ and $K_{\lfloor \frac{N}{2} \rfloor} < 0$, (31) has local minima only when the phases are in the splay state, i.e., when the N phases are evenly distributed around S^1. Fig. 3 shows two simulation examples of patterns of five moving particles that were stabilized using the control laws (25) and (26) with these potentials. Note that the two patterns shown in Fig. 3(a) and (b) are stabilized for particle systems with identical speed profiles and control laws but different frequencies Ω and ω.

Remark 1. The phase potential stabilization relies upon the condition that $\dot{\theta}_k = \omega$ and $\dot{\phi}_k = \Omega$ for each $k = 1, \ldots, N$ at steady state, i.e., we require homogeneous natural frequencies in heading and speed. By removing U, V, or both from the control, we eliminate the need for the corresponding homogeneity. Therefore, if we do not desire

to stabilize a specific phase arrangement either in heading or speed, we may allow the individual natural frequencies to be independent.

Remark 2. In [7] we showed that, for sinusoidal speed, control for the kth particle can be calculated from relative heading measurements, its position relative to the center of mass of the group, and its speed and rate of change of speed relative to the group average.

V. CONCLUSION

In this paper we derive expressions for the trajectories of steered particles with periodically time-varying speed and constant turning rate in steady state. Conditions are given for boundedness of the trajectories, and bounds on the variation from a circular orbit are described. We derive control laws to stabilize systems of such particles to corresponding motion patterns and provide examples that may be of interest for multi-agent sampling applications. The results are for all-to-all communication, although the limited communication generalizations of [5] should be adaptable to the current setting. It is of interest to further consider the application of the results presented here to mobile sampling networks, both to enable efficient collective sensing in vehicle networks and to understand the periodic speed variation observed in fish schools [7].

REFERENCES

[1] F. Zhang and N. Leonard, "Cooperative control and filtering for cooperative exploration." To appear in *IEEE Trans. Automatic Control*, 2008.

[2] E. Justh and P. Krishnaprasad, "Equilibria and steering laws for planar formations," *Systems and Control Letters*, vol. 52, pp. 25–38, 2004.

[3] T. Vicsek, A. Czirók, E. Ben-Jacob, I. Cohen, O. Shochet, and A. Tenenbaum, "Novel type of phase transition in a system of self-driven particles," *Phys. Rev. Lett.*, vol. 75, pp. 1226–1229, 1995.

[4] A. Jadbabaie, J. Lin, and A. Morse, "Coordination of groups of mobile autonomous agents using nearest neighbor rules," *IEEE Trans. Automatic Control*, vol. 48, no. 6, pp. 988–1001, 2003.

[5] R. Sepulchre, D. Paley, and N. Leonard, "Stabilization of planar collective motion with limited communication," *IEEE Trans. Automatic Control*, vol. 53, no. 3, pp. 706–719, 2008.

[6] I. Couzin, J. Krause, R. James, G. Ruxton, and N. Franks, "Collective memory and spatial sorting in animal groups," *J. Theor. Biology*, no. 218, pp. 1–11, 2002.

[7] D. Swain, N. Leonard, I. Couzin, A. Kao, and R.J.Sepulchre, "Alternating spatial patterns for coordinated group motion," in *Proc. 46th IEEE Conf. on Decision and Control*, December 2007.

[8] D. Swain, M.Cao, and N.E.Leonard, "Effective sensing regions and connectivity of agents undergoing periodic relative motions," in *Proc. 47th IEEE Conf. on Decision and Control*, 2008.

[9] D. J. Klein and K. A. Morgansen, "Controlled collective motion for trajectory tracking," in *Proc. 2006 American Control Conf.*, 2006.

[10] E. Lalish, K. A. Morgansen, and T. Tsukamaki, "Oscillatory control for constant-speed unicycle-type vehicles," in *Proc. 46th IEEE Conf. on Decision and Control*, 2007.

[11] D. Paley, F. Zhang, and N. Leonard, "Cooperative control for ocean sampling: The glider coordinated control system," *IEEE Trans. Control Systems Technology*, vol. 16, no. 4, pp. 735–744, 2008.

[12] Y. Kuramoto, *Chemical oscillations, waves, and turbulence*. Springer-Verlag, 1984.

[13] S. Watanabe and S. Strogatz, "Constants of motion for superconductor arrays," *Physica D*, vol. 74, pp. 197–253, 1994.

[14] R. Sepulchre, D. Paley, and N. Leonard, "Stabilization of planar collective motion: All-to-all communication," *IEEE Trans. Automatic Control*, vol. 52, no. 5, pp. 811–824, 2007.

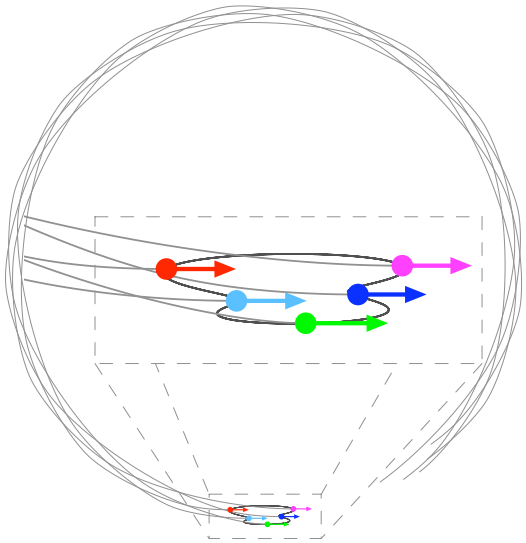

(a)

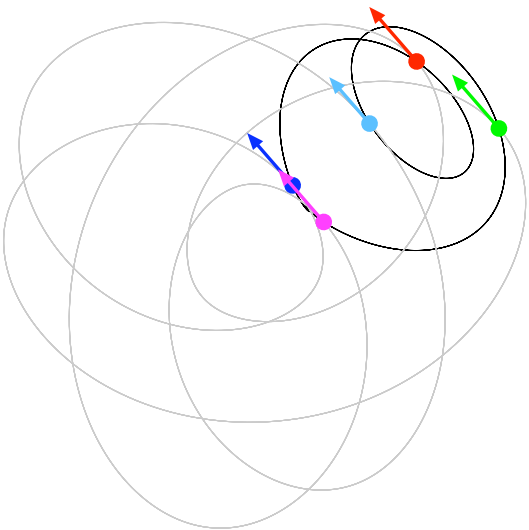

(b)

Fig. 3. Sample patterns generated by five particles with speed profiles of the form shown in Fig. 2(a). (a) With $\Omega = \pi$ and $\omega = 0.3\pi$ (yielding the same q_k as Fig. 2(b)) (b) With $\Omega = 0.6\pi$ and $\omega = \pi$. In both figures, the controls (25) and (26) were used with the heading phase potential U given by (30), $\kappa_\theta = -0.1$, the speed phase potential V given by (31), $\kappa_\phi = 0.1$, and $\kappa_c = 1$, yielding synchronized headings and evenly spaced speed phases in steady state. In both figures the particle trajectories are shown in light gray, the q_k shape is shown in black, and the particle locations and headings are indicated by the colored arrows. In (a) the inset magnifies the particle locations and pattern.